Environmental Science & Technology

Article

pubs.acs.org/est

# Arsenic(V) Incorporation in Vivianite during Microbial Reduction of Arsenic(V)-Bearing Biogenic Fe(III) (Oxyhydr)oxides

E. Marie Muehe,*[,†,∥] Guillaume Morin,[‡] Lukas Scheer,[†] Pierre Le Pape,[‡] Imène Esteve,[‡] Birgit Daus,[§] and Andreas Kappler[†]

[†]Geomicrobiology, Center for Applied Geosciences, University of Tuebingen, Tuebingen, Germany

[‡]Environmental Mineralogy, Institut de Minéralogie, de Physique des Matériaux et de Cosmochimie (IMPMC), UMR7590 - CNRS - UPMC, 75252, Paris cedex 05, France

[§]UFZ – Helmholtz Centre for Environmental Research, Department Analytical Chemistry, Leipzig, Germany

Supporting Information

**ABSTRACT:** The dissolution of arsenic-bearing iron(III) (oxyhydr)oxides during combined microbial iron(III) and arsenate(V) reduction is thought to be the main mechanism responsible for arsenic mobilization in reducing environments. Besides its mobilization during bioreduction, arsenic is often resequestered by newly forming secondary iron(II)-bearing mineral phases. In phosphate-bearing environments, iron(II) inputs generally lead to vivianite precipitation. In fact, in a previous study we observed that during bioreduction of arsenate(V)-bearing biogenic iron(III) (oxyhydr)oxides in phosphate-containing growth media, arsenate(V) was immobilized by the newly forming secondary iron(II) and iron(II)/iron(III)mineral phases, including vivianite. In the present study, changes in arsenic redox state and binding environment in these experiments were analyzed. We found that arsenate(V) partly replaced phosphate in vivianite, thus forming a vivianite-symplesite solid solution identified as $Fe_3(PO_4)_{1.7}(AsO_4)_{0.3}{\cdot}8H_2O$. Our data suggests that in order to predict the fate of arsenic during the bioreduction of abiogenic and biogenic iron(III) (oxyhydr)oxides in arsenic-contaminated environments, the formation of symplesite–vivianite minerals needs to be considered. Indeed, such mineral phases could contribute to a delayed and slow release of arsenic in phosphate-bearing surface and groundwater environments.

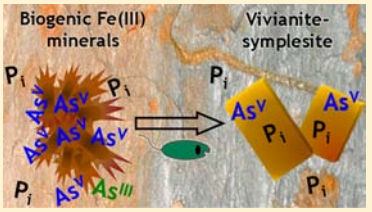


## INTRODUCTION

Arsenic (As) is one of the most widely studied metalloids since it has been recognized as a major threat to human health, especially when present at concentrations above the recommended WHO levels (10 $\mu g\ L^{-1}$) in groundwater aquifers.[1,2] Elevated aqueous As concentrations as found in the aquifers of Bengal and Mekong deltas are caused by a combination of various geochemical and microbial processes.[1−3] The transformation of As-bearing minerals during their riverine transport from Himalaya leads to the binding of As to Fe(III) (oxyhydr)oxide minerals within the deltaic sediments.[4−6] Arsenic may then be released from the surface of these Fe(III) minerals by sorption competitors, such as phosphate,[7] bicarbonate,[8] silicic acid,[9] natural organic matter (NOM, e.g., humic substances)[10,11] as well as by the formation of mobile humic–Fe–As complexes and colloidal aggregates.[12,13] Additionally, microbial reduction of the mineral-bound As(V) to the more mobile As(III) form was suggested to lead to As mobilization.[14−17] The most important factor responsible for the high As concentrations in the groundwater, however, is thought to be related to reductive dissolution of the As-bearing Fe(III) (oxyhydr)oxide minerals by Fe(III)-reducing bacteria in anoxic As-contaminated aquifers.[16,18] By using allochthonous and autochthonous organic matter these bacteria reductively dissolve Fe(III) (oxyhydr)oxides, leading to the release of the bound As.[2−4,18,19] The feasibility of this process was also simulated with long-time column experiments, in which As release was accompanied by the progressive export of aqueous Fe(II) from the columns.[20,21]

Fe(III) (oxyhydr)oxides in the environment are formed either via chemical or microbial oxidation of Fe(II).[22,23] Biogenic Fe(III) (oxyhydr)oxides have been found in various environments[24−30] and were typically associated with cell-derived organic matter.[31−35] Organic carbon and ion impurities hinder homogeneous crystal growth,[22] leading to smaller and less crystalline biogenic minerals compared to abiogenic Fe(III) (oxyhydr)oxides.[36−39] Phosphate is one such ion impurity and is thus frequently encountered as a major constituent of Fe(III) (oxyhydr)oxides found in many different environmental systems.[40−45] Bacteriogenic Fe(III) (oxyhydr)oxides were shown to be highly susceptible to microbial reduction compared to synthetic, poorly crystalline Fe phase analogues, though the rate of bioreduction varied according to the mineralogy of the biogenic Fe(III) (oxyhydr)oxide.[46,47] The resulting biogenic Fe(II) mineral products able to capture As include siderite ($FeCO_3$),[48] magnetite ($Fe^{II}Fe^{III}{}_2O_4$),[20,48−50] green rust ($Fe^{II}{}_4Fe^{III}{}_2(OH)_{12}CO_3$),[51] and vivianite

Received: September 21, 2015
Revised: January 29, 2016
Accepted: February 1, 2016
Published: February 1, 2016





DOI: 10.1021/acs.est.5b04625
Environ. Sci. Technol. 2016, 50, 2281−2291

$(Fe_3(PO_4)_2)$[48,49] in batch and short-time column experiments. Especially vivianite is of interest as secondarily formed Fe(II) mineral phase in culture media,[47,48] aquifers,[52] and in fertilized and nonfertilized paddy soils.[53,54] More specifically, Islam et al.[48] showed that vivianite sorbs As(V) after bioreduction of soluble Fe(III) but did not observe direct evidence for As(V) incorporation in the vivianite structure. More recently, Muehe et al.[46] found that microbial reduction of As(V)-bearing biogenic Fe(III) (oxyhydr)oxides in freshwater medium containing 1 mM phosphate resulted mainly in the formation of vivianite. They discussed that As(V) is very likely to be associated with vivianite but so far, the mechanism of As(V) immobilization during this process is unknown.

The goal of the present study was to investigate the fate of As after microbial reduction of As(V)-bearing biogenic Fe(III) (oxyhydr)oxides. More specifically, the objectives were (I) to identify the localization and binding mode of As(V) and As(III) in the newly formed Fe mineral phases using electron microscopy and synchrotron-based X-ray absorption spectroscopy and (II) to identify arsenic speciation changes in the solid and liquid phase to better understand the mobility of As in the system. The presentation of the data will conclude to the discussion of the mechanisms of As scavenging and release processes under the reducing conditions investigated.

## MATERIAL AND METHODS

**Source of Microorganism, Microbial Growth Conditions, And Biogenic Fe(III) (Oxyhydr)oxide Synthesis.** We used the Fe(III)-reducing $\gamma$-proteobacterium *Shewanella oneidensis* strain MR-1, which utilizes a wide range of organic substrates and uses Fe(III) as an electron acceptor in the absence of $O_2$.[55] Iron-free precultures (20 mM lactate, 40 mM fumarate) and experimental cultures (20 mM lactate, 5−7 mM Fe(III) biogenic minerals) of strain MR-1 were grown in freshwater medium (0.14 g $L^{-1}$ $KH_2PO_4$, 0.2 g $L^{-1}$ NaCl, 0.3 g $L^{-1}$ $NH_4Cl$, 0.5 g $L^{-1}$ $MgSO_4 \cdot 7H_2O$, 0.1 g $L^{-1}$ $CaCl_2 \cdot 2H_2O$, 22 mM bicarbonate buffer, pH 7, 1 mL $L^{-1}$ vitamin solution, 1 mL $L^{-1}$ trace element solution, 1 mL $L^{-1}$ selenate-tungstate solution) and prepared under an $N_2/CO_2$ (80/20 v/v) atmosphere according to Muehe et al.[46] The biogenic material used in the experiments here was produced independently of the Muehe et al.[46] study, as large quantities of minerals were needed for analysis. However, these experiments were run at the same time when the Muehe et al.[46] study was performed, using the same chemicals, apparatuses, and incubators, ensuring maximum compliance between both studies. As the geochemical, XRD, and microscopic data of this study and Muehe et al.[46] are in accordance, we assume that the mineralogy of the here-used biogenic material is the same as in Muehe et al.[46]

The As(V)-bearing biogenic Fe(III) (oxyhydr)oxides were synthesized using *Acidovorax* sp. strain BoFeN1 according to Hohmann et al.[56] and Muehe et al.,[46] and harvested and processed according to Muehe et al.[46] Biogenic Fe(III) minerals with two initial Fe(III) to As(V) ratios of 250 to 1 and of 50 to 1 [w/w] were investigated, which approximates to 335 to 1 and 67 to 1 [Fe mol/As mol] or 0.003 to 1 and 0.015 to 1 [As mol/Fe mol], respectively.

For Fe(III) reduction experiments with strain MR-1, 50 mL of freshwater medium were setup in 100 mL bottles and amended with 5−7 mM of As-bearing biogenic Fe(III) minerals, 20 mM of Na−lactate, and 100 $\mu$M of 9,10-anthraquinone-2,6-disulfonate (AQDS). 2 $\times 10^5$ cells $mL^{-1}$ of strain MR-1 were added to the set-ups from an iron-free preculture grown on 20 mM lactate as electron donor and 40 mM fumarate as electron acceptor. The synthesis of the biogenic Fe(III) (oxyhydr)oxide and their reduction with MR-1 were performed in the dark at 28 °C. Aqueous and solid-phase samples were taken at the end of the microbial exponential growth phase after 5 days of reduction to ensure the analysis of freshly formed and nonaged secondary Fe(II) minerals according to Muehe et al.[46]

## SAMPLING OF BATCH EXPERIMENTS

All experiments were conducted in triplicate. Samples were taken anoxically in a $N_2$-filled glovebox before and after inoculation with strain MR-1 as well as after 5 days. For each time point, three parallel individual bottles were sampled for determining the solution chemistry followed by harvesting the minerals for mineralogical analyses. Aqueous samples were taken with anoxic syringes and analyzed for total and dissolved Fe(II) and Fe(III), total dissolved As and As speciation according to Muehe et al.[46] Samples for quantification of total dissolved As were frozen at −20 °C until measurement. The minerals were harvested in the glovebox by decanting the supernatant followed by centrifugation (13 200*g* for 2 min) and vacuum drying of the mineral pellet. Once dry, the minerals of three parallel bottles were pooled in equal amounts for mineral analysis.

**Solution Chemistry Analysis.** Total and dissolved Fe(II) and Fe(III) were quantified spectro-photometrically using the ferrozine assay according to Stookey, 1970[57] and following the protocol in Muehe et al.[46] While Fe(II) was directly quantified with the ferrozine assay, Fe(III) was first reduced by 10% hydroxylamine hydrochloride before determining total Fe by complexation with ferrozine. Total dissolved As was quantified by diluting thawed samples in 2% $HNO_3$ and measuring with an inductively coupled-plasma mass-spectrometer (7700 series ICP-MS, Agilent Technologies). Using a high-pressure-liquid chromatography-coupled ICP-MS (7700 series ICP-MS, Agilent Technologies), the As redox speciation present before and after incubation were quantified in a 10 mM phosphoric acid matrix, which preserves the redox state of As.[58]

**Mineralogical and Spectroscopic Analyses.** All samples for mineral and Fe−As bonding environment analysis were prepared under anoxic conditions in glove boxes or bags, dried under vacuum, and stored and transported anoxically in the dark. Samples were only exposed to ambient air when taken out of the anoxic transporting container followed by direct insertion into the analytical device. The mineralogy and the binding environment, location, and speciation of Fe and As in the minerals present before (0 day) and during microbial Fe(III) reduction (day 5) were investigated using powder X-ray diffraction (XRD), scanning electron microscopy (SEM) combined with energy dispersive X-ray spectrometry (EDXS), as well as with X-ray absorption near-edge structure (XANES) and extended X-ray absorption fine structure (EXAFS) spectroscopy at the Fe and As K-edge.

XRD patterns were acquired using an X'Pert pro Panalytical Diffractometer equipped with an X'celerator detector. Samples were deposited on a zero-background Si sample holder and loaded into an anoxic sample chamber equipped with a curved Kapton window (constructed by the IMPMC project group). Data were collected over the 5−80° two-theta range with a 0.017° two-theta step, counting 4 h per sample. Spectra were interpreted using the ICSD database for goethite (#15-9970), vivianite (#20-0703), and siderite (#68298).


DOI: 10.1021/acs.est.5b04625
*Environ. Sci. Technol.* 2016, 50, 2281−2291

**Table 1. Concentrations and Redox Speciation of Total and Aqueous Fe and Aqueous As after 0 and 5 Days of Reduction of As(V)-Bearing Biogenic Fe(III) Minerals by *Shewanella oneidensis* strain MR-1[a]**

| | Fe | | | aqueous As | | |
|---|---|---|---|---|---|---|
| | total Fe(II) [mM] [%] | aqu. Fe(tot) [mM] [%] | aqu. Fe(II) [mM] [%] | [mg $L^{-1}$] | As(V) [%] | As(III) [%] |
| Fe to As(V) Ratio 250 mg:1 mg (total Fe = 5–6 mM) | | | | | | |
| MR-1 inoculated | | | | | | |
| 0 days | 0.39 ± 0.07 | 0.02 ± 0.01 | 0.02 ± 0.00 | 0.30 ± 0.01 | 92.7 ± 1.0 | 7.3 ± 1.0 |
| | 6.8 ± 1.8 | 0.4 ± 0.2 | 0.4 ± 0.1 | | | |
| 5 days | 1.75 ± 0.10 | 0.87 ± 0.05 | 0.70 ± 0.07 | 0.40 ± 0.00 | 66.1 ± 0.8 | 33.9 ± 0.8 |
| | 34.9 ± 2.0 | 17.2 ± 1.0 | 14.0 ± 1.3 | | | |
| Fe to As(V) Ratio 50 mg:1 mg (total Fe = 6–7 mM) | | | | | | |
| MR-1 inoculated | | | | | | |
| 0 days | 0.58 ± 0.09 | 0.05 ± 0.01 | 0.03 ± 0.00 | 1.39 ± 0.07 | 96.3 ± 0.6 | 3.7 ± 0.6 |
| | 8.6 ± 0.4 | 0.7 ± 0.3 | 0.4 ± 0.1 | | | |
| 5 days | 3.24 ± 0.09 | 1.07 ± 0.15 | 0.99 ± 0.18 | 0.90 ± 0.04 | 66.2 ± 2.0 | 33.8 ± 2.0 |
| | 53.0 ± 0.6 | 17.6 ± 2.2 | 16.1 ± 2.6 | | | |

[a]Biogenic Fe(III) (oxyhydr)oxides initially contained two different concentrations of As(V) with Fe to As(V) ratios of 250:1 and 50:1 (w/w). Given is the range for total Fe present in each setup. For each setup and time point total Fe(II) in mM and in % of total Fe, aqueous Fe(total) and Fe(II) in mM and in % of total Fe, aqueous As in mg $L^{-1}$ differentiating between As(V) and As(III) in % of aqueous As are shown. Data is given as the average value and its standard deviation considering triplicates for each time point. Each sample per setup was measured thrice for Fe and twice for As. Abiotic controls were monitored in parallel to biological setups and are not depicted in the table for simplicity, but remained below 8% for total Fe(II) and below 1% for dissolved Fe(tot) and Fe(II).

SEM analyses of carbon-coated samples were performed with a Zeiss ultraTM 55 electron microscope operating at 10 kV with a 60 $\mu$m diaphragm in high current mode. Secondary electron images were obtained with an in-lens detector and EDXS analyses were collected using a Bruker Si-drift detector. The As/Fe and P/Fe molar ratio for specific mineral phases were determined by averaging 10 consecutive spot measurements per mineral phase. Semiquantitative analyses and elemental mapping was performed with the program Esprit 1.8(3) using a spectra database for standard materials. Raw EDX elemental maps were built using the integrated intensities of the Fe L$\alpha$, P K$\alpha$, and As L$\alpha$ emission lines. EDXS spectra were plotted for selected areas by averaging the spectra recorded for the corresponding pixels. Background subtracted EDX elemental maps were calculated via semiquantitative elemental analysis using the background subtracted intensities of the Fe L$\alpha$, P K$\alpha$, and As K$\alpha$ emission lines in individual EDX spectra obtained by binning the mapping data over four pixels.

X-ray absorption spectroscopy (XAS) data at the Fe K-edge were collected in transmission detection mode below 20K using a He cryostat on the SAMBA beamline at SOLEIL, Orsay, France. Arsenic K-edge data were collected in fluorescence detection mode using a 30 element Ge detector on the FAME-BM30B beamline at ESRF, Grenoble, France. Data for the As:vivianite model compound were collected in fluorescence detection mode using a 38 element Ge array detector on the SAMBA beamline. In order to minimize the photoreduction of As under the X-ray beam, all As K-edge data were recorded below 20K using a He cryostat and the focused beam (<0.3 $mm^2$) was moved 1 mm on the sample between each EXAFS scan (Supporting Information (SI) Figure S1). Data were averaged, normalized, and background-subtracted using the Athena program.[59] XANES and EXAFS data were least-squares fitted by a linear combination of appropriate model compound spectra, using a classical Levenberg-Marquart algorithm. Spectra components for these fits were selected from a large database of model compound spectra. Our Fe K-edge spectra database includes ferric (oxyhydr)oxides[56,60] and/or ferrous hydroxides and oxides,[61,62] phosphates,[40,62] sulfates,[63] and carbonates.[64] Our As K-edge spectra database includes numerous As(V) and As(III) minerals[63] as well as a large variety of As sorption samples on Fe minerals, see refs 56, 65, 66 and references therein. In addition, for the present study an As(V)-substituted vivianite sample, referred to as As:vivianite, was synthesized by modifying the protocol for vivianite synthesis given by Eynard et al.[67] A final As/P molar ratio of 1 mol % was aimed at. For this, As-bearing vivianite was synthesized at room temperature in a $N_2$-filled anoxic glovebox, by neutralizing a 250 mL mixture of 0.035 M $H_3PO_4$ and 0.05 M $FeSO_4$ in the presence of As(V) (27.5 mg of $HAsNa_2O_4{\cdot}7H_2O$) in $O_2$-free deionized water (final As to ($As+PO_4$) ratio of 1 mol %). The solution was slowly neutralized to pH 6 using a 0.05 M KOH solution while stirring. Once the pH was stabilized, the solution was gently stirred for an hour. The resulting solid was recovered after settling, centrifugation (15 min, 6500 rpm), and washing 3 times in 10 mL of Milli-Q water before vacuum drying in the anoxic glovebox. The mineralogical purity of the synthesized As-bearing vivianite was checked by XRD (data not shown).

The relative accuracy on the LCF components is estimated to 10% and detection limit to 5%.[68,69]

## RESULTS

**Aqueous Geochemistry of Fe and As during Microbial Reduction of As(V)-Bearing Fe(III) (Oxyhydr)oxides.** Strain MR-1 efficiently reduced the As(V)-loaded biogenic Fe(III) (oxyhydr)oxides with an initial Fe to As ratios of 250:1 and 50:1 (w/w) leading to the formation of 1.8 ± 0.1 mM and 3.2 ± 0.1 mM of total Fe(II) after 5 days, corresponding to 34.9 ± 2.0% and 53.0 ± 0.6% of the total iron, respectively (Table 1). Approximately 50% and 33% of the formed Fe(II) remained in the aqueous phase of the setups with initial Fe to As ratios of 250:1 and 50:1 (w/w), respectively, while the rest was present



DOI: 10.1021/acs.est.5b04625
Environ. Sci. Technol. 2016, 50, 2281–2291

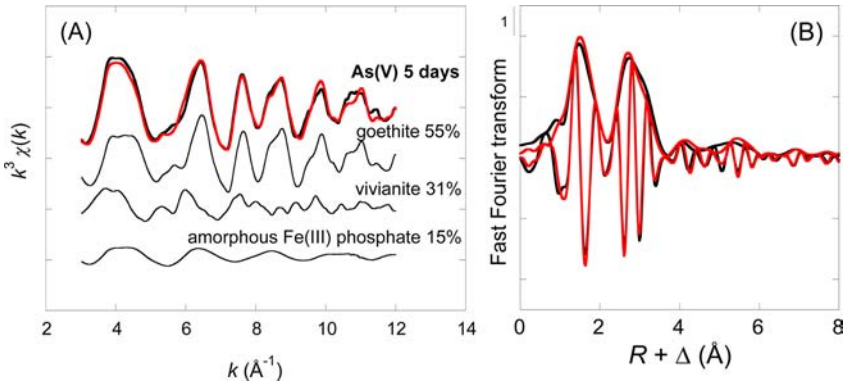


**Figure 1.** Fe K-edge EXAFS (A) and their corresponding Fast Fourier Transform (B) of As(V)-bearing biogenic Fe(III) minerals with a Fe to As(V) ratio of 50 to 1 w/w that were reduced by *Shewanella oneidensis* strain MR-1 for 5 days. The black line on top of A and in B represent the measured data set, whereas the red lines depict the fitted graphs obtained by linear combination of the underlying references according to their stated percentages. Standard deviation on the fitted proportions is ±4% and components below 10% are considered as not significant.[68]

in solid form. Total Fe(II) in the sterile controls was below 8% of total initial iron throughout the experiment (data not shown).

Total aqueous As concentrations increased by 0.1 mg $L^{-1}$ to 0.4 ± 0.0 mg $L^{-1}$ from the beginning of the incubation until 5 days for the setup with an Fe to As ratio of 250:1 (w/w), with 34% of the aqueous As(V) being reduced to As(III) (Table 1). Total aqueous As concentrations for the setup with a Fe to As ratio of 50:1 decreased from 1.4 ± 0.1 mg $L^{-1}$ to 0.9 ± 0.0 mg $L^{-1}$ within the first 5 days, with 34% of the aqueous As being in the form of As(III).

**Mineralogical Composition of the Solids.** For some of the mineralogical analyses the As content was too low in the setup with a Fe to As ratio of 250 to 1, therefore we provide all data only for the 50:1 system and some data for the 250:1 system. After 5 days of microbial reduction of the As(V)-bearing biogenic Fe(III) (oxyhydr)oxides, XRD analysis indicated that a significant fraction of the initial mineral phase goethite [$\alpha$-FeOOH] still remained and that the minerals vivianite [$Fe_3(PO_4)_2{\cdot}8H_2O$] and siderite [$FeCO_3$] were formed (SI Figure S2). No magnetite [$Fe_3O_4$] was detected based on XRD analysis. The relative proportion of vivianite to the biogenic goethite/ferrihydrite starting mineral could not be reliably determined using Rietveld analysis of the XRD patterns (SI Figure S3) because of a significant preferential orientation of the vivianite platelets, especially for the sample with a Fe to As ratio of 50 to 1 (w/w). The unit-cell parameters of vivianite in the incubated samples and of the 1 wt % As(V)-substituted vivianite model compound fell within the range of cell-parameters reported for vivianite and symplesite [$Fe_3(AO_4)_2{\cdot}8H_2O$] (SI Table S1). Results of the Linear Combination Fit (LCF) analysis of the Fe K-edge EXAFS data for the experiment conducted with an initial Fe to As ratio of 50:1 (w/w) are displayed in Figure 1. These results show that 55 ± 4% of the initially present poorly crystalline goethite phase was reduced, forming 31 ± 4% vivianite of the solid Fe pool after 5 days of microbial incubation. An additional minor amorphous Fe(III) phosphate phase of 15% was present after 5 days of microbial Fe(III) reduction.

**Localization of As and P in Mineral Aggregates.** SEM observations showed the abundant presence of vivianite crystals of ~5 $\mu$m in size with a platelet-like shape after 5 days of incubation (Figure 2a). The white arrow in Figure 2a indicates the potential remains of a *S. oneidensis* MR-1 cell within a

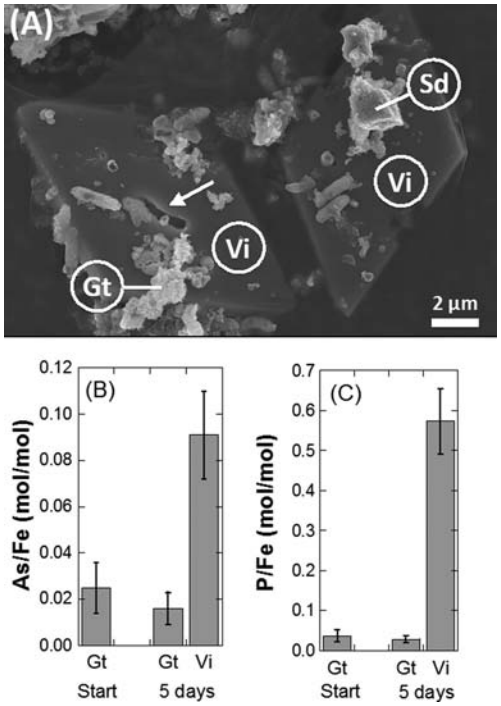


**Figure 2.** (A) Scanning electron micrograph of a sample collected after 5 days of reduction of As(V)-bearing biogenic Fe(III) (oxyhydr)oxides (Fe to As ratio of 50 to 1 w/w) showing vivianite crystals (Vi), biogenic Fe(III) (oxyhydr)oxides most similar to goethite (Gt), siderite crystals (Sd), and *Shewanella oneidensis* strain MR-1 cells. The white arrow indicates the remaining shape of a *S. oneidensis* cell associated with the mineral phase. (B) As to Fe ratios and (C) P to Fe ratios for the minerals goethite (Gt) and vivianite (Vi) at the start of the experiment and after 5 days of Fe(III) reduction by strain MR-1 using energy dispersive X-ray spot spectroscopy. Values are given in the arbitrary units mol % per mol %, mean ± sd, $n$ = 10.

vivianite precipitate. The initial solid phases, consisting of mineral-encrusted cells, and bulbous mineral material, had previously been identified as a poorly crystalline goethite/ferrihydrite mix[56] and were systematically observed under SEM in the samples collected throughout the experiment (Figure 2a), in agreement with XRD and Fe K-edge EXAFS data. According to EDX microanalyses, this initial goethite/ferrihydrite mineral phase had an As/Fe mole ratio of 0.02 ± 0.01 that did not vary significantly throughout the experiment


DOI: 10.1021/acs.est.5b04625
Environ. Sci. Technol. 2016, 50, 2281−2291

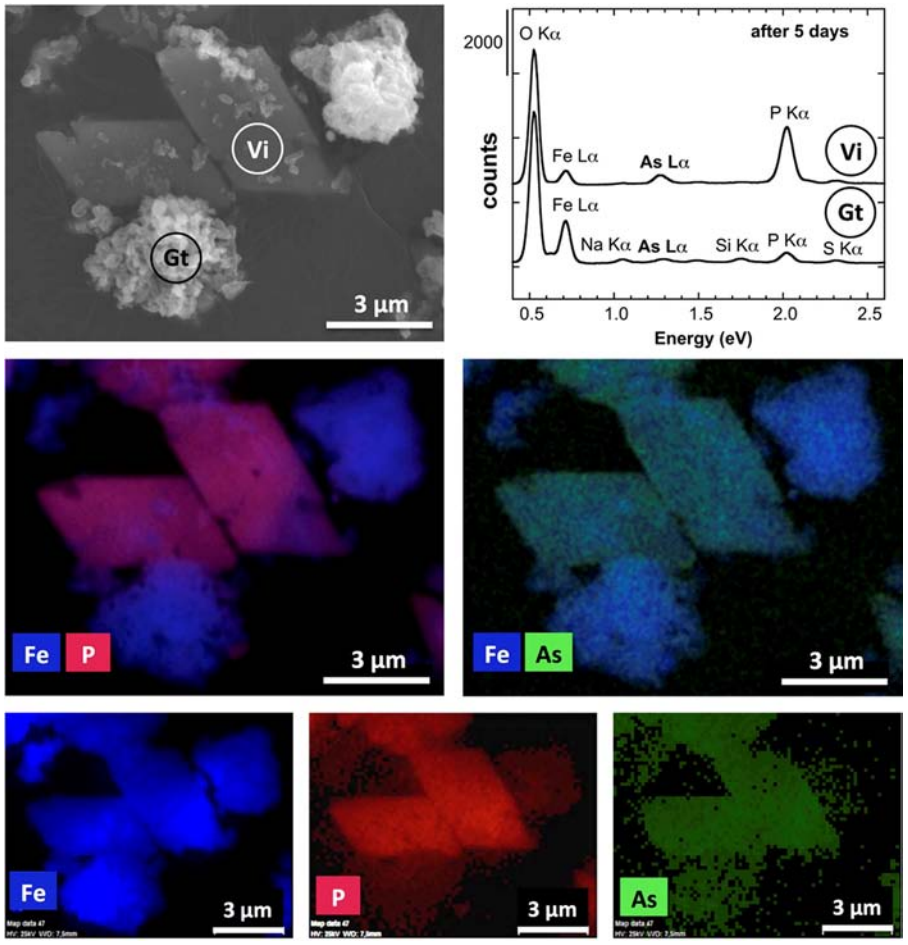


**Figure 3.** Energy dispersive X-ray spectroscopy analysis of a representative scanning electron microscopy image (EDX-SEM map) of As(V)-bearing biogenic Fe(III) minerals that were reduced by *Shewanella oneidensis* strain MR-1 for 5 days. Biogenic Fe(III) (oxyhydr)oxides initially contained As(V) with an Fe to As(V) ratio of 50 to 1 w/w. (Upper left) secondary electron image of biogenic Fe(III) mineral goethite (Gt) and the reduction product vivianite (Vi), (Upper right) average EDX spectra extracted from the circled areas in the map correspond to vivianite platelets (Vi) and goethite encrusted bacteria (Gt). (Center left) raw EDX map for Fe in blue and for P in red, (Center right) raw EDX map for Fe in blue and for As in green. (Lower panel from left to right) background-subtracted EDX maps for Fe, P, and As.

(Figure 2b). The ratio of 0.02 fits well to the calculated ratio of 0.015 for the initial substrate (see Materials and Methods section). EDX analyses of the samples incubated for 5 days (Figures 2a and 3) indicated that the forming vivianite platelet-shaped mineral phase had a P/Fe molar ratio of 0.58 ± 0.10 (Figure 2c). Interestingly, EDX elemental mapping showed that this phase contained a significant amount of As (Figure 3) and semiquantitative analyses of EDX spectra indicated an As/Fe molar ratio of 0.09 ± 0.03 in this vivianite phase (Figure 2b). In addition, cube-shaped siderite crystals were scarcely observed, as indicated by weak Bragg peak intensities in the XRD patterns. The low number of isolated siderite particles prevented any statistically satisfying analysis of their elemental composition using SEM-EDX. Including siderite as a fitting component in our LCF analysis of the Fe K-edge EXAFS data did not improve the fits, suggesting that this phase was present at concentrations below the detection limit of this method, that is, 5−10% of the total Fe in the samples.

**Redox State and Binding Environment of As.** XANES (Figure 4) and EXAFS (Figure 5) data at the As K-edge were analyzed using a similar LCF procedure as used for the Fe K-edge XAS data (results reported in Table 2). Best linear combination Fits of the EXAFS data at the As K-edge for the incubated samples were obtained using As(V)-sorbed to goethite, As(III)-sorbed to ferrihydrite, and the As(V)-vivianite model compound as fitting components (Table 2; Figure 5). These components were also used as fitting components for XANES data (Table 2; Figure 4). Discrepancies between XANES and EXAFS results fell within uncertainties (Table 2). XANES LCF results indicated that the proportion of As(III) over total As was lower than 10% in the initial goethite/ferrihydrite mineral phase with an Fe to As ratio of 50 to 1 (w/w) (Figure 4a). This proportion increased to ∼40% after 5 days of incubation.

$AsO_4$ for $PO_4$ substitution in the 1 wt % As(V)-substituted vivianite model compound was demonstrated by a good agreement between the observed As−Fe distances and coordination numbers determined by shell-by-shell analysis of the EXAFS spectrum of this reference sample (SI Figure S4; Table S2), with the local structure of vivianite (SI Figure S5), assuming a slight relaxation of the structure (SI Table S2). This shell-by-shell analysis revealed contributions from long distance multiple scattering paths within the structure that appear as high frequency signal in the unfiltered EXAFS spectrum of this model compound (Figure 5B; SI Figure S4). Fitting the EXAFS spectra without including this As(V)-substituted vivianite


DOI: 10.1021/acs.est.5b04625
*Environ. Sci. Technol.* 2016, 50, 2281−2291

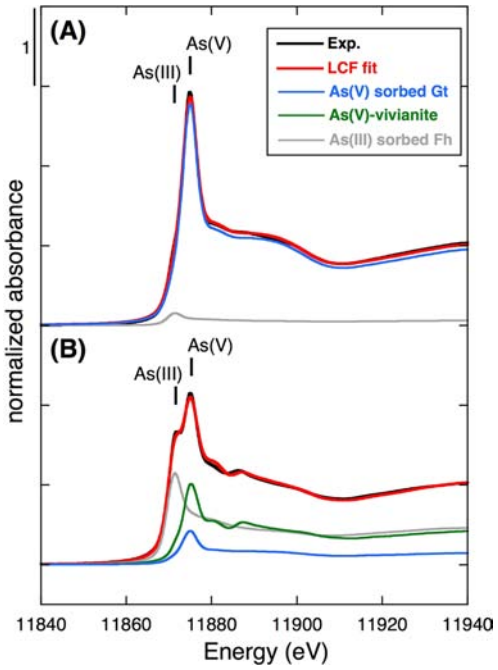


**Figure 4.** As K-edge XANES of As(V)-bearing biogenic Fe(III) minerals with a Fe to As(V) ratio of 50 to 1 (w/w) that were reduced by *Shewanella oneidensis* strain MR-1 at time points 0 (A) and 5 days (B). Experimental and linear combination fit curves are plotted as black and red lines, respectively. Spectral components weighted by their fitted proportions reported in Table 2 are As(V) sorbed on goethite (blue line); As(III) sorbed on ferrihydrite (gray line); As(V):vivianite (green line).

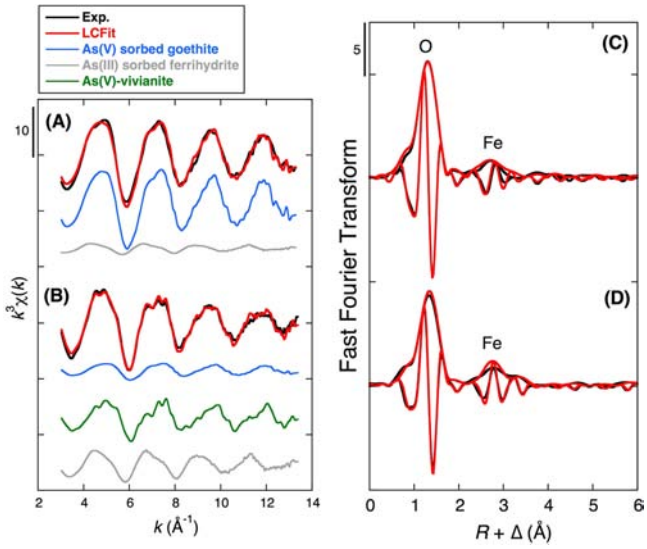


**Figure 5.** As $k^3$-weighted EXAFS (A, B) and their corresponding Fast Fourier Transform (C, D) of As(V)-bearing biogenic Fe(III) minerals with a Fe to As(V) ratio of 50:1 (w/w) that were reduced by *Shewanella oneidensis* strain MR-1 at time points 0 (A, C) and 5 days (B, D). Experimental and linear combination fit curves are plotted as black and red lines, respectively. Spectral components weighted by their fitted proportions reported in the Table 2 are As(V) sorbed on goethite (blue line); As(III) sorbed on ferrihydrite (gray line); As(V):vivianite (green line).

component yielded significant discrepancies between the matching spectral features (SI Figure S6A).

LCF analysis of the EXAFS spectra for these samples indicated that the As(III) component could be fitted by As(III)-sorbed to ferrihydrite, thus indicating that As(III) was mainly sorbed to the surface of the initial goethite/ferrihydrite phase, both in the starting materials and after 5 days of incubation. Alternative fits using As(III)-sorbed to goethite instead of As(III)-sorbed to ferrihydrite yielded acceptable results but with a higher residue (SI Figure S6C). However, a minor contribution of As(III) sorbed on the surface of siderite or vivianite could not be excluded. XANES and EXAFS LCF also indicated that a significant proportion of As remained as As(V) sorbed to the goethite/ferrihydrite mineral phase (Figure 5a, b), accounting for approximately ~15% for the 5 day sample.

Importantly, XANES (Figure 4) and EXAFS (Figure 5) LCF results (Table 2) for the samples collected after 5 days indicated that ~40% of the total As in the solid phase was in the form of $AsO_4^{3-}$ anions substituting for $PO_4^{3-}$ in the structure of vivianite, thus forming a solid-solution between vivianite and symplesite ($Fe_3(AsO_4)_2 \cdot 8H_2O$), with an approximate structural formula $[Fe_3(PO_4)_{1.7}(AsO_4)_{0.3} \bullet 8H_2O]$, as indicated by SEM-EDX analyses (Figure 2b,c).

## DISCUSSION

Microbial reduction of As-bearing Fe(III) (oxyhydr)oxides does not necessarily lead to mineral dissolution and mobilization of the associated As, but can also lead to the formation of secondary Fe(II) (e.g., siderite, vivianite) and mixed Fe(II)/Fe(III) (e.g., magnetite, green rust) mineral phases that are able to resequester As.[20,46,48,50,70] For most of these Fe minerals, their mode of interaction with As is well-described in the literature, with the exception of vivianite. For instance, magnetite[65,70−73] and to a lesser extent, green-rusts[66,72,74] have been demonstrated to sorb As(V) and As(III). The extent of As sorption to siderite is generally limited, with As(V) showing an inner-sphere sorption behavior, which is stronger than the observed outer-sphere sorption of As(III) to siderite.[72] In the present study we show that during microbial reduction of As(V)-bearing biogenic Fe(III) (oxyhydr)oxides in pH-neutral freshwater medium with a 1 mM phosphate content As can be scavenged by coprecipitation with vivianite. Consequently, the following discussion focuses on the formation of secondarily formed As(V)-bearing vivianite. We then discuss the impact of As(V) to As(III) reduction on the mobility of As in this system.

**As(V) Sequestration into Vivianite.** Our previous study on the microbial reduction of As-loaded biogenic Fe(III) (oxyhydr)oxides[46] in combination with the present study suggests that As(V) is initially mobilized and then immobilized by the formation of secondary Fe minerals (Figure 6b−e). The presence of medium-derived phosphate, whose concentration was approximately 10-fold higher compared to typical concentrations found in aquifers[75] and paddy fields,[76] thus influences the formation of vivianite. In addition, medium-derived phosphate competed for As(V) sorption onto the Fe (oxyhydr)oxide surfaces, and thus, displaced some As(V) from these mineral surfaces before Fe(III) reduction started (Figure 6a and Muehe et al.[46]). Such early mobilized As(V) could engage in mineral precipitation reactions right from the start of the experiment.

The present study shows that a significant fraction of the As in form of As(V) ions substitutes for phosphate in the structure of vivianite, as demonstrated by a combination of SEM-EDX


DOI: 10.1021/acs.est.5b04625
Environ. Sci. Technol. 2016, 50, 2281−2291

**Table 2. Results of the Linear Combination Fitting (LCF) of the As K-edge XANES and EXAFS of the As(V)-Bearing Biogenic Fe(III) Minerals with a Fe to As(V) Ratio of 50 to 1 w/w that Were Reduced by *Shewanella oneidensis* Strain MR-1 for 5 days[a]**

| sample | LCF | As(V)/goethite | As(III)/ferrihydrite | As(V):vivianite | Sum | *R*-factor ($\times 10^4$) |
|---|---|---|---|---|---|---|
| 0 days | XANES | 93(12) | 6(4) | | 99 | 3.8 |
| | EXAFS | 80(5) | 15(5) | | 96 | 251 |
| 5 days | XANES | 14(6) | 43(15) | 42(14) | 99 | 3.6 |
| | EXAFS | 17(6) | 43(2) | 40(6) | 100 | 259 |

[a]The proportions of the fitted components are given in % with the uncertainties of the last digit shown in brackets. Contributions below 5% are not significant.[69] The goodness of fit is estimated by *R*-factor = $\sum (y_{calc} - y_{exp})^2 / \sum y_{exp}^2$.

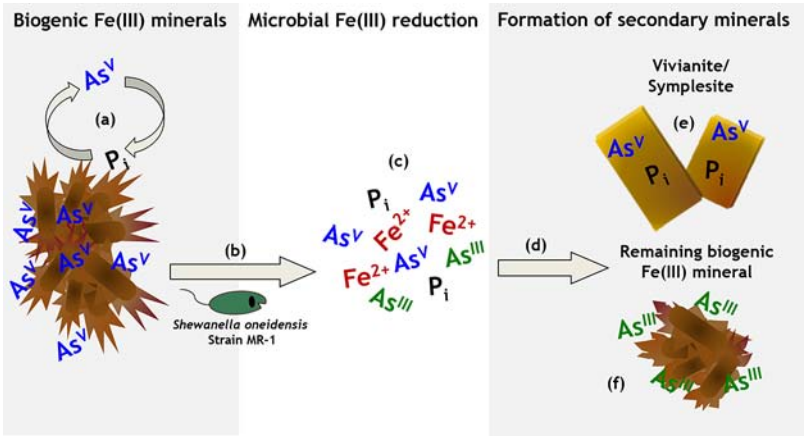


**Figure 6.** Scheme summarizing the fate and binding environment of As during microbial reduction of As(V)-bearing biogenic Fe(III) (oxyhydr)oxides. As(V) bound to the surface of biogenic Fe(III) (oxyhydr)oxides is in equilibrium with aqueous As(V) due to competitive replacement by phosphate ($P_i$) that is present in the microbial growth medium (a). Upon microbial Fe(III) reduction by *Shewanella oneidensis* strain MR-1 (b), dissolved $Fe^{2+}$ and As are present (c). $Fe^{2+}$ precipitates slowly into the secondary Fe mineral vivianite (d). During the formation of vivianite aqueous As(V) could substitute for $P_i$ forming symplesite (e). Mobilized As(III) binds effectively to the remaining biogenic Fe(III) (oxyhydr)oxide mineral phase (f).

data (Figure 2) and EXAFS analysis using a reference compound for As-substituted vivianite (Table 1 and Figure 5). As shown by Frost et al.[77] such isomorphic substitution is expected to be readily possible since the thermochemical radius of phosphate (2.38 Å) and arsenate (2.48 Å) are close[78] and vivianite ($Fe_3(PO_4)_2 \cdot 8H_2O$) and symplesite ($Fe_3(AsO_4)_2 \cdot 8H_2O$) are isostructural minerals.[79] Considering the respective As/Fe and P/Fe ratios of ~0.08 and 0.58 obtained with SEM-EDX in our study, the biogenically formed mixed Fe−As/P mineral phase is shifted more toward the phosphate end member rather than to the As(V) one, with the following approximate structural formula $Fe_3(PO_4)_{1.75}(AsO_4)_{0.25} \cdot 8H_2O$. The solubility products of symplesite and vivianite at 25 °C are very similar to $10^{-33.25}$ and $10^{-33.06}$ $mol^2\ L^{-2}$, respectively,[80] which suggests that a vivianite-symplesite solid solution might also have a similar solubility product. This mixed phase could form even when the solution would be under-saturated for each individual end-member (i.e., for either symplesite or vivianite), but as soon as the ion activity product (calculated using the sum of the individual arsenate and phosphate concentrations) exceeds the estimated solubility product of the mixed vivianite-symplesite solid. This calculation using the present phosphate and arsenate concentrations actually showed that the saturation for the mixed vivianite-symplesite was reached with a saturation index of 17.7 in our experiments and therefore precipitation of a mixed As−P−Fe(II) mineral phase was expected based on solubility product calculations (the full calculation is provided in the SI Table S3). Harvey et al.[52] actually calculated vivianite to be supersaturated from their measured aqueous concentrations in Bangladeshi aquifers, and also observed this mineral phase by scanning electron microscopy as rims on host grains. However, they did not specifically look for the incorporation of As in this phase. Supportingly, Johnston and Singer, 2007[80] modeled that symplesite could actually form in reduced, $Fe^{2+}$-rich, pH-neutral As-contaminated aquifers in Southeast Asia, and could potentially play an important role as an Fe(II) and As(V) sink under anoxic conditions. The present study suggests that solid solutions of the two minerals could also form in such reducing environments as well as in fertilized flooded rice paddies, and would thus favor As(V) scavenging, provided that the phosphate activity would be high enough (Figure 6e). In fact, the formation of vivianite particles has been shown convincingly on rice roots grown on $P_2O_5$-fertilized soil in pot experiments,[53] and paddy fields.[54] To our knowledge, the formation of As-bearing vivianite in paddy fields or even the presence of As in vivianite particles around rice roots has not been investigated yet, and would certainly be of interest.

**As Redox Transformation at the Fe(III) (Oxyhydr)-oxide Surface Influences As Mobilization.** In the present study, As(V) reduction occurred as evidenced by increasing aqueous and solid phase As(III) concentrations during and after microbial Fe(III) reduction. Indeed, before microbial Fe(III) reduction started, some of the As was already present in solution and consisted mainly of As(V). Phosphate in the medium and organics as constituents of the biogenic Fe(III) minerals probably displace some As(V) from Fe(III) (oxyhydr)oxide surfaces (Figure 6a) as they compete for the same sorption sites with As(V).[7,11] A loss of As from these


DOI: 10.1021/acs.est.5b04625
Environ. Sci. Technol. 2016, 50, 2281−2291

biogenic Fe(III) minerals is supportingly evidenced by decreasing As to Fe ratios in the biogenic goethite/ferrihydrite mineral phase during microbial Fe(III) reduction. Once microbial Fe(III) reduction started (Figure 6b), As(V) was reduced to As(III) that accounted for up to 40% of the total As in both the aqueous and solid phases (Tables 1 and 2, Figure 6c).

Some *Shewanella* strains are known to be capable of dissimilatory Fe(III) and/or aqueous and mineral-bound As(V) reduction,[14,50,81] but not strain MR-1 that was used in the present study. Indeed, control experiments with *S. oneidensis* strain MR-1 have confirmed that under the here-applied conditions, strain MR-1 was not able to reduce aqueous As(V) directly in the presence of freshwater medium, 40 mM fumarate, 20 mM lacetate, and in the absence of AQDS (SI Figure S7). However, we setup the present Fe(III) (oxyhydr)-oxide reduction microcosms in the presence of 100 $\mu$M of AQDS, which strain MR-1 reduces intermediately to $AH_2QDS$ to shuttle electrons to Fe(III) mineral phases.[82−84] This reduced form of AQDS has been shown by Jiang et al.[83] to be able to reduce approximately 10% of the As(V) present to As(III) at circumneutral pH. However, Jiang et al.[83] used 5-fold less of the electron donor $AH_2QDS$ than As(V), whereas in our study either equal concentrations or 4-fold more AQDS than As(V) was present in the setups with Fe to As ratios of 50 to 1 or 250 to 1, respectively. We therefore repeated these control experiments to quantify As(V) reduction by $AH_2QDS$ under our experimental conditions. We did not observe any significant reduction of As(V) by $AH_2QDS$ within 5 days of incubation (SI Figure S8) and thus the exact mechanism of As(V) reduction in our experiments remains unknown.

The reduction of As(V) by reactive Fe(II) (i.e., mineral-sorbed Fe(II)) is unlikely since As(V) to As(III) reduction has not been observed in the presence of green-rust, magnetite and siderite[66,72] nor in the presence of Fe(II)-sorbed goethite.[85]

Despite the significant reduction of As(V) to As(III), the proportion of total aqueous As did not vary considerably over the course of incubation (Table 1), that is, As was not released significantly. This could be due to binding of As(III) to the fraction of the initial goethite-ferrihydrite mineral phase that remained even after reduction, which was observed by EXAFS analysis showing efficient inner-sphere sorption of As(III) to the initial goethite-ferrihydrite minerals remaining after reduction. This observation is in agreement with the high affinity of As(III) for ferric (oxyhydr)oxide surfaces at neutral pH (Figure 6f) that was also previously observed.[73] By comparison, As(III) does not bind well to vivianite.[86]

**Environmental Implications.** In the present study, we demonstrate that As(V) can readily replace phosphate in slowly forming phosphate-containing Fe(II) minerals during reductive transformation of As-loaded biogenic Fe(III) (oxyhydr)oxides forming mixed arsenate/phosphate Fe(II) mineral phases. Such vivianite-symplesite mixed mineral phases could be of environmental relevance as they could form in circumneutral, anoxic, $Fe^{2+}$- and phosphate-bearing As-bearing aquifers and sediments.[78] In fact, Harvey et al.[52] reported that Bangladeshi aquifers contain 0.1−0.3 w% of amorphous Fe potentially present as ferrous phosphates, which could contain As. This would translate to approximately 0.04−0.1 w% of P in vivianite and thus 0.005−0.016 w% of As. Furthermore, vivianite-symplesite mineral phases could also be of environmental relevance for rice cultivation in As-contaminated rice paddies as Nanyzo et al.[53] quantified 2.0−4.5 g P $kg^{-1}$ dry rice roots as vivianite. This vivianite could thus contain 0.29−0.64 g As $kg^{-1}$ dry root. Whether these vivianite-symplesite mineral phases occur in these environments, how stable they are, whether and how fast As(V) can be leached out of them, whether they pose a potential pool for a delayed or prolonged release of As in aquifers or reduce the uptake of As by rice, needs to be further investigated. To fully understand the mobilization and sequestration of As in contaminated environments, the potential presence and formation of vivianite/symplesite mixed mineral phases needs to be considered especially in phosphate and/or organic matter rich environments.

## ■ ASSOCIATED CONTENT

### Supporting Information

The Supporting Information is available free of charge on the ACS Publications website at DOI: 10.1021/acs.est.5b04625.

Figures, S1−S8, and Tables, S1−S3 (PDF)

## ■ AUTHOR INFORMATION


### Corresponding Author

*Phone: +1-650-291-9715, e-mail: mmuehe@stanford.edu.

### Present Address

‖(E.M.M.) Environmental Soil Biogeochemistry, Earth System Science, Stanford University, Stanford, California 94305, United States.


### Notes

The authors declare no competing financial interest.

## ■ ACKNOWLEDGMENTS

We thank Dr. Joern Breuer and Baerbel Horn (LAChemie Universitaet Hohenheim for ICP-MS analysis. We are indebted to the FAME beamline staff at ESRF, Jean-Louis Hazemann, Olivier Proux, Isabelle Kieffer, Denis Testemale, and Eric Lahera and as well as to the SAMBA beamline staff at SOLEIL, Emiliano Fonda, Valérie Briois and Stéphanie Belin, and Laurent Barthe for their precious help during XAS data collection. We also acknowledge the IMPMC Project group for conception and maintenance of the anoxic XRD chamber (Frédéric Gélébart, Ludovic Delbes, Benoit Baptiste). We thank Region IdF, CNRS and UPMC for funding of the SEM and XRD facilities IMPMC. This work was supported by the scholarship program of the German Federal Environmental Foundation to E. Marie Muehe.

## ■ REFERENCES


(1) Smedley, P. L.; Kinniburgh, D. G. A review of the source, behaviour and distribution of arsenic in natural waters. *Appl. Geochem.* **2002**, *17* (5), 517−568.

(2) Muehe, E. M.; Kappler, A. Arsenic mobility and toxicity in the environment − a review on biogeochemistry, health and socio-economic effects, remediation and future predictions. *Environ. Chem.* **2014**, *11*, 483−495.

(3) Fendorf, S.; Michael, H. A.; van Geen, A. Spatial and temporal variations of groundwater arsenic in South and Southeast Asia. *Science* **2010**, *328* (5982), 1123−1127.

(4) Nickson, R.; McArthur, J.; Burgess, W.; Ahmed, K. M.; Ravenscroft, P.; Rahman, M. Arsenic poisoning of Bangladesh groundwater. *Nature* **1998**, *395* (6700), 338−338.

(5) Das, D.; Samanta, G.; Mandal, B. K.; Chowdhury, T. R.; Chanda, C. R.; Chowdhury, P. P.; Basu, G. K.; Chakraborti, D. Arsenic in groundwater in six districts of West Bengal, India. *Environ. Geochem. Health* **1996**, *18* (1), 5−15.




DOI: 10.1021/acs.est.5b04625
*Environ. Sci. Technol.* 2016, 50, 2281−2291

(6) Chowdhury, T. R.; Basu, G. K.; Mandal, B. K.; Biswas, B. K.; Samanta, G.; Chowdhury, U. K.; Chanda, C. R.; Lodh, D.; Lal Roy, S.; Saha, K. C.; Roy, S.; Kabir, S.; Quamruzzaman, Q.; Chakraborti, D. Arsenic poisoning in the Ganges delta. *Nature* **1999**, *401* (6753), 545−546.
(7) Acharyya, S. K.; Chakraborty, P.; Lahiri, S.; Raymahashay, B. C.; Guha, S.; Bhowmik, A. Arsenic poisoning in the Ganges delta. *Nature* **1999**, *401* (6753), 545−545.
(8) Appelo, C. A. J.; Van der Weiden, M. J. J.; Tournassat, C.; Charlet, L. Surface complexation of ferrous iron and carbonate on ferrihydrite and the mobilization of arsenic. *Environ. Sci. Technol.* **2002**, *36* (14), 3096−3103.
(9) Swedlund, P. J.; Webster, J. G. Adsorption and polymerisation of silicic acid on ferrihydrite, and its effect on arsenic adsorption. *Water Res.* **1999**, *33* (16), 3413−3422.
(10) Redman, A. D.; Macalady, D. L.; Ahmann, D. Natural organic matter affects arsenic speciation and sorption onto hematite. *Environ. Sci. Technol.* **2002**, *36* (13), 2889−2896.
(11) Bauer, M.; Blodau, C. Mobilization of arsenic by dissolved organic matter from iron oxides, soils and sediments. *Sci. Total Environ.* **2006**, *354* (2−3), 179−190.
(12) Sharma, P.; Ofner, J.; Kappler, A. Formation of binary and ternary colloids and dissolved complexes of organic matter, Fe and As. *Environ. Sci. Technol.* **2010**, *44* (12), 4479−4485.
(13) Sharma, P.; Rolle, M.; Kocar, B.; Fendorf, S.; Kappler, A. Influence of natural organic matter on As transport and retention. *Environ. Sci. Technol.* **2011**, *45* (2), 546−553.
(14) Oremland, R. S.; Stolz, J. F. The ecology of arsenic. *Science* **2003**, *300* (5621), 939−944.
(15) Lear, G.; Song, B.; Gault, A. G.; Polya, D. A.; Lloyd, J. R. Molecular analysis of arsenate-reducing bacteria within Cambodian sediments following amendment with acetate. *Appl. Environ. Microbiol.* **2007**, *73* (4), 1041−1048.
(16) Rowland, H. A. L.; Boothman, C.; Pancost, R.; Gault, A. G.; Polya, D. A.; Lloyd, J. R. The role of indigenous microorganisms in the biodegradation of naturally occurring petroleum, the reduction of iron, and the mobilization of arsenite from West Bengal aquifer sediments. *J. Environ. Qual.* **2009**, *38* (4), 1598−1607.
(17) Héry, M.; van Dongen, B. E.; Gill, F.; Mondal, D.; Vaughan, D. J.; Pancost, R. D.; Polya, D. A.; Lloyd, J. R. Arsenic release and attenuation in low organic carbon aquifer sediments from West Bengal. *Geobiology* **2010**, *8* (2), 155−168.
(18) Islam, F. S.; Gault, A. G.; Boothman, C.; Polya, D. A.; Charnock, J. M.; Chatterjee, D.; Lloyd, J. R. Role of metal-reducing bacteria in arsenic release from Bengal delta sediments. *Nature* **2004**, *430* (6995), 68−71.
(19) McArthur, J. M.; Ravenscroft, P.; Safiulla, S.; Thirlwall, M. F. Arsenic in groundwater: Testing pollution mechanisms for sedimentary aquifers in Bangladesh. *Water Resour. Res.* **2001**, *37* (1), 109−117.
(20) Tufano, K. J.; Fendorf, S. Confounding impacts of iron reduction on arsenic retention. *Environ. Sci. Technol.* **2008**, *42* (13), 4777−4783.
(21) Fakih, M.; Davranche, M.; Dia, A.; Nowack, B.; Morin, G.; Petitjean, P.; Chatellier, X.; Gruau, G. Environmental impact of As (V)−Fe oxyhydroxide reductive dissolution: An experimental insight. *Chem. Geol.* **2009**, *259* (3), 290−303.
(22) Cornell, R. M.; Schwertmann, U. *The Iron Oxides: Structure, Properties, Reactions, Occurences and Uses*, 2nd ed.; Wiley-VCH GmbH & Co. KGaA: Weinheim, Germany, 2003.
(23) Konhauser, K. O.; Kappler, A.; Roden, E. E. Iron in microbial metabolisms. *Elements* **2011**, *7* (2), 89−93.
(24) Clarke, W. A.; Konhauser, K. O.; Thomas, J. C.; Bottrell, S. H. Ferric hydroxide and ferric hydroxysulfate precipitation by bacteria in an acid mine drainage lagoon. *FEMS Microbiol. Rev.* **1997**, *20* (3−4), 351−361.
(25) Konhauser, K. O.; Jones, B.; Reysenbach, A. L.; Renaut, R. W. Hot spring sinters: keys to understanding Earth's earliest life forms. *Can. J. Earth Sci.* **2003**, *40* (11), 1713−1724.
(26) Fortin, D.; Davis, B.; Southam, G.; Beveridge, T. J. Biogeochemical phenomena induced by bacteria within sulfidic mine tailings. *J. Ind. Microbiol.* **1995**, *14* (2), 178−185.
(27) Ferris, F. G.; Beveridge, T. J.; Fyfe, W. S. Iron-silica crystallite nucleation by bacteria in a geothermal sediment. *Nature* **1986**, *320* (6063), 609−611.
(28) Ferris, F. G.; Konhauser, K. O.; Lyven, B.; Pedersen, K. Accumulation of metals by bacteriogenic iron oxides in a subterranean environment. *Geomicrobiol. J.* **1999**, *16* (2), 181−192.
(29) Hegler, F.; Losekann-Behrens, T.; Hanselmann, K.; Behrens, S.; Kappler, A. Influence of seasonal and geochemical changes on the geomicrobiology of an iron carbonate mineral water spring. *Appl. Environ. Microbiol.* **2012**, *78* (20), 7185−7196.
(30) Posth, N.; Canfield, D. E.; Kappler, A. Biogenic Fe(III) minerals: From formation to diagenesis and preservation in the rock record. *Earth-Sci. Rev.* **2014**, *135*, 103−121.
(31) Posth, N. R.; Huelin, S.; Konhauser, K. O.; Kappler, A. Size, density and composition of cell-mineral aggregates formed during anoxygenic phototrophic Fe(II) oxidation: Impact on modern and ancient environments. *Geochim. Cosmochim. Acta* **2010**, *74* (12), 3476−3493.
(32) Hohmann, C.; Winkler, E.; Morin, G.; Kappler, A. Anaerobic Fe(II)-oxidizing bacteria show As resistance and immobilize As during Fe(III) mineral precipitation. *Environ. Sci. Technol.* **2010**, *44* (1), 94−101.
(33) Chan, C. S.; De Stasio, G.; Welch, S. A.; Girasole, M.; Frazer, B. H.; Nesterova, M. V.; Fakra, S.; Banfield, J. F. Microbial polysaccharides template assembly of nanocrystal fibers. *Science* **2004**, *303* (5664), 1656−1658.
(34) Schädler, S.; Burkhardt, C.; Hegler, F.; Straub, K. L.; Miot, J.; Benzerara, K.; Kappler, A. Formation of cell-iron-mineral aggregates by phototrophic and nitrate-reducing anaerobic Fe(II)-oxidizing bacteria. *Geomicrobiol. J.* **2009**, *26* (2), 93−103.
(35) Emerson, D.; Revsbech, N. P. Investigation of an iron-oxidizing microbial mat community located near Aarhus, Denmark - laboratory studies *Appl. Environ. Microbiol.* **1994**, *60*(11), 4032−4038
(36) Fortin, D.; Ferris, F. G. Precipitation of iron, silica, and sulfate on bacterial cell surfaces. *Geomicrobiol. J.* **1998**, *15* (4), 309−324.
(37) Kappler, A.; Schink, B.; Newman, D. K. Fe(III) mineral formation and cell encrustation by the nitrate-dependent Fe(II)-oxidizer strain BoFeN1. *Geobiology* **2005**, *3* (4), 235−245.
(38) Ferris, F. G.; Hallberg, R. O.; Lyven, B.; Pedersen, K. Retention of strontium, cesium, lead and uranium by bacterial iron oxides from a subterranean environment. *Appl. Geochem.* **2000**, *15* (7), 1035−1042.
(39) Kappler, A.; Newman, D. K. Formation of Fe(III)-minerals by Fe(II)-oxidizing photoautotrophic bacteria. *Geochim. Cosmochim. Acta* **2004**, *68* (6), 1217−1226.
(40) Cosmidis, J.; Benzerara, K.; Morin, G.; Busigny, V.; Lebeau, O.; Jezequel, D.; Noel, V.; Dublet, G.; Othmane, G. Biomineralization of iron-phosphates in the water column of Lake Pavin (Massif Central, France). *Geochim. Cosmochim. Acta* **2014**, *126*, 78−96.
(41) Buffle, J.; De Vitre, R. R.; Perret, D.; Leppard, G. G. Physico-chemical characteristics of a colloidal iron phosphate species formed at the oxic-anoxic interface of a eutrophic lake. *Geochim. Cosmochim. Acta* **1989**, *53* (2), 399−408.
(42) Hongve, D. Cycling of iron, manganese, and phosphate in a meromictic lake. *Limnol. Oceanogr.* **1997**, *42* (4), 635−647.
(43) Lienemann, C.-P.; Monnerat, M.; Dominik, J.; Perret, D. Identification of stoichiometric iron-phosphorus colloids produced in a eutrophic lake. *Aquat. Sci.* **1999**, *61* (2), 133−149.
(44) Dellwig, O.; Leipe, T.; März, C.; Glockzin, M.; Pollehne, F.; Schnetger, B.; Yakushev, E. V.; Böttcher, M. E.; Brumsack, H.-J. A new particulate Mn−Fe−P-shuttle at the redoxcline of anoxic basins. *Geochim. Cosmochim. Acta* **2010**, *74* (24), 7100−7115.
(45) Gunnars, A.; Blomqvist, S.; Johansson, P.; Andersson, C. Formation of Fe(III) oxyhydroxide colloids in freshwater and brackish seawater, with incorporation of phosphate and calcium. *Geochim. Cosmochim. Acta* **2002**, *66* (5), 745−758.


DOI: 10.1021/acs.est.5b04625
*Environ. Sci. Technol.* 2016, 50, 2281−2291

(46) Muehe, E. M.; Scheer, L.; Daus, B.; Kappler, A. Fate of arsenic during microbial reduction of biogenic vs. abiogenic As-Fe(III)-mineral co-precipitates. *Environ. Sci. Technol.* **2013**, *47*, 8297−8307.
(47) Langley, S.; Gault, A.; Ibrahim, A.; Renaud, R.; Fortin, D.; Clark, I. D.; Ferris, F. G. A comparison of the rates of Fe(III) reduction in synthetic and bacteriogenic iron oxides by *Shewanella putrefaciens* CN32. *Geomicrobiol. J.* **2009**, *26* (2), 57−70.
(48) Islam, F. S.; Pederick, R. L.; Gault, A. G.; Adams, L. K.; Polya, D. A.; Charnock, J. M.; Lloyd, J. R. Interactions between the Fe(III)-reducing bacterium *Geobacter sulfurreducens* and arsenate, and capture of the metalloid by biogenic Fe(II). *Appl. Environ. Microbiol.* **2005**, *71* (12), 8642−8648.
(49) Glasauer, S.; Weidler, P. G.; Langley, S.; Beveridge, T. J. Controls on Fe reduction and mineral formation by a subsurface bacterium. *Geochim. Cosmochim. Acta* **2003**, *67* (7), 1277−1288.
(50) Kocar, B. D.; Herbel, M. J.; Tufano, K. J.; Fendorf, S. Contrasting effects of dissimilatory iron(III) and arsenic(V) reduction on arsenic retention and transport. *Environ. Sci. Technol.* **2006**, *40* (21), 6715−6721.
(51) Ona-Nguema, G.; Morin, G.; Wang, Y.; Menguy, N.; Juillot, F.; Olivi, L.; Aquilanti, G.; Abdelmoula, M.; Ruby, C.; Bargar, J. R. Arsenite sequestration at the surface of nano-$Fe(OH)_2$, ferrous-carbonate hydroxide, and green-rust after bioreduction of arsenic-sorbed lepidocrocite by *Shewanella putrefaciens*. *Geochim. Cosmochim. Acta* **2009**, *73* (5), 1359−1381.
(52) Harvey, C. F.; Swartz, C. H.; Badruzzaman, A. B. M.; Keon-Blute, N.; Yu, W.; Ali, M. A.; Jay, J.; Beckie, R.; Niedan, V.; Brabander, D.; Oates, P. M.; Ashfaque, K. N.; Islam, S.; Hemond, H. F.; Ahmed, M. F. Arsenic mobility and groundwater extraction in Bangladesh. *Science* **2002**, *298* (5598), 1602−1606.
(53) Nanzyo, M.; Yaginuma, H.; Sasaki, K.; Ito, K.; Aikawa, Y.; Kanno, H.; Takahashi, T. Identification of vivianite formed on the roots of paddy rice grown in pots. *Soil Sci. Plant Nutr.* **2010**, *56* (3), 376−381.
(54) Nanzyo, M.; Onodera, H.; Hasegawa, E.; Ito, K.; Kanno, H. Formation and dissolution of vivianite in paddy field soil. *Soil Sci. Soc. Am. J.* **2013**, *77* (4), 1452−1459.
(55) Myers, C. R.; Nealson, K. H. Bacterial manganese reduction and growth with manganese oxide as the sole electron-acceptor. *Science* **1988**, *240* (4857), 1319−1321.
(56) Hohmann, C.; Morin, G.; Ona-Nguema, G.; Guigner, J. M.; Brown, G. E.; Kappler, A. Molecular-level modes of As binding to Fe(III) (oxyhydr)oxides precipitated by the anaerobic nitrate-reducing Fe(II)-oxidizing *Acidovorax* sp strain BoFeN1. *Geochim. Cosmochim. Acta* **2011**, *75* (17), 4699−4712.
(57) Stookey, L. L. Ferrozine-a new spectrophotometric reagent for iron. *Anal. Chem.* **1970**, *42* (7), 779−781.
(58) Daus, B.; Mattusch, J.; Wennrich, R.; Weiss, H. Investigation on stability and preservation of arsenic species in iron rich water samples. *Talanta* **2002**, *58* (1), 57−65.
(59) Ravel, B.; Newville, M. ATHENA, ARTEMIS, HEPHAESTUS: data analysis for X-ray absorption spectroscopy using IFEFFIT. *J. Synchrotron Radiat.* **2005**, *12* (4), 537−541.
(60) Maillot, F.; Morin, G.; Wang, Y.; Bonnin, D.; Ildefonse, P.; Chaneac, C.; Calas, G. New insight into the structure of nanocrystalline ferrihydrite: EXAFS evidence for tetrahedrally coordinated iron(III). *Geochim. Cosmochim. Acta* **2011**, *75* (10), 2708−2720.
(61) Pantke, C.; Obst, M.; Benzerara, K.; Morin, G.; Ona-Nguema, G.; Dippon, U.; Kappler, A. Green rust formation during Fe(II) oxidation by the nitrate-reducing *Acidovorax* sp strain BoFeN1. *Environ. Sci. Technol.* **2012**, *46* (3), 1439−1446.
(62) Baumgartner, J.; Morin, G.; Menguy, N.; Perez Gonzalez, T.; Widdrat, M.; Cosmidis, J.; Faivre, D. Magnetotactic bacteria form magnetite from a phosphate-rich ferric hydroxide via nanometric ferric (oxyhydr)oxide intermediates. *Proc. Natl. Acad. Sci. U. S. A.* **2013**, *110* (37), 14883−8.
(63) Maillot, F.; Morin, G.; Juillot, F.; Bruneel, O.; Casiot, C.; Ona-Nguema, G.; Wang, Y.; Lebrun, S.; Aubry, E.; Vlaic, G. Structure and reactivity of As (III)-and As (V)-rich schwertmannites and amorphous ferric arsenate sulfate from the Carnoulès acid mine drainage, France: Comparison with biotic and abiotic model compounds and implications for As remediation. *Geochim. Cosmochim. Acta* **2013**, *104*, 310−329.
(64) Dublet, G.; Juillot, F.; Morin, G.; Fritsch, E.; Noel, V.; Brest, J.; Brown, G. E. XAS evidence for Ni sequestration by siderite in a lateritic Ni-deposit from New Caledonia. *Am. Mineral.* **2014**, *99* (1), 225−234.
(65) Wang, Y.; Morin, G.; Ona-Nguema, G.; Juillot, F.; Calas, G.; Brown, G. E., Jr Distinctive arsenic (V) trapping modes by magnetite nanoparticles induced by different sorption processes. *Environ. Sci. Technol.* **2011**, *45* (17), 7258−7266.
(66) Wang, Y.; Morin, G.; Ona-Nguema, G.; Juillot, F.; Guyot, F.; Calas, G.; Brown, G. E., Jr Evidence for different surface speciation of arsenite and arsenate on green rust: an EXAFS and XANES study. *Environ. Sci. Technol.* **2009**, *44* (1), 109−115.
(67) Eynard, A.; Del Campillo, M. C.; Barrón, V.; Torrent, J. Use of vivianite ($Fe_3(PO_4)_2.8H_2O$) to prevent iron chlorosis in calcareous soils. *Fert. Res.* **1992**, *31* (1), 61−67.
(68) O'Day, P. A.; Rivera, N.; Root, R.; Carroll, S. A. X-ray absorption spectroscopic study of Fe reference compounds for the analysis of natural sediments. *Am. Mineral.* **2004**, *89* (4), 572−585.
(69) Cances, B.; Juillot, F.; Morin, G.; Laperche, V.; Alvarez, L.; Proux, O.; Hazemann, J.-L.; Brown, G. E.; Calas, G. XAS evidence of As (V) association with iron oxyhydroxides in a contaminated soil at a former arsenical pesticide processing plant. *Environ. Sci. Technol.* **2005**, *39* (24), 9398−9405.
(70) Wang, Y.; Morin, G.; Ona-Nguema, G.; Brown, G. E. Arsenic (III) and Arsenic (V) speciation during transformation of lepidocrocite to magnetite. *Environ. Sci. Technol.* **2014**, *48* (24), 14282−14290.
(71) Wang, Y. H.; Morin, G.; Ona-Nguema, G.; Menguy, N.; Juillot, F.; Aubry, E.; Guyot, F.; Calas, G.; Brown, G. E. Arsenite sorption at the magnetite-water interface during aqueous precipitation of magnetite: EXAFS evidence for a new arsenite surface complex. *Geochim. Cosmochim. Acta* **2008**, *72* (11), 2573−2586.
(72) Jonsson, J.; Sherman, D. M. Sorption of As(III) and As(V) to siderite, green rust (fougerite) and magnetite: Implications for arsenic release in anoxic groundwaters. *Chem. Geol.* **2008**, *255* (1−2), 173−181.
(73) Dixit, S.; Hering, J. G. Comparison of arsenic(V) and arsenic(III) sorption onto iron oxide minerals: Implications for arsenic mobility. *Environ. Sci. Technol.* **2003**, *37* (18), 4182−4189.
(74) Randall, S. R.; Sherman, D. M.; Ragnarsdottir, K. V. Sorption of As(V) on green rust ($Fe_4(II)Fe_2(III)(OH)_{12}SO_4{\cdot}3H_2O$) and lepidocrocite ($\gamma$-FeOOH): Surface complexes from EXAFS spectroscopy. *Geochim. Cosmochim. Acta* **2001**, *65* (7), 1015−1023.
(75) Meng, X.; Korfiatis, G. P.; Christodoulatos, C.; Bang, S. Treatment of arsenic in Bangladesh well water using a household co-precipitation and filtration system. *Water Res.* **2001**, *35* (12), 2805−2810.
(76) Dittmar, J.; Voegelin, A.; Maurer, F.; Roberts, L. C.; Hug, S. J.; Saha, G. C.; Ali, M. A.; Badruzzaman, A. B. M.; Kretzschmar, R. Arsenic in soil and irrigation water affects arsenic uptake by rice: Complementary insights from field and pot studies. *Environ. Sci. Technol.* **2010**, *44* (23), 8842−8848.
(77) Frost, R. L.; Martens, W.; Williams, P. A.; Kloprogge, J. T. Raman spectroscopic study of the vivianite arsenate minerals. *J. Raman Spectrosc.* **2003**, *34* (10), 751−759.
(78) Da Silva, J. J. R. F.; Williams, R. J. P. *The Biological Chemistry of the Elements: The Inorganic Chemistry of Life*, 1st ed.; Oxford University Press: Oxford, 1997.
(79) Mori, H.; Ito, T. The structure of vivianite and symplesite. *Acta Crystallogr.* **1950**, *3* (1), 1−6.
(80) Johnston, R. B.; Singer, P. C. Solubility of symplesite (ferrous arsenate): Implications for reduced groundwaters and other geochemical environments. *Soil Sci. Soc. Am. J.* **2007**, *71* (1), 101−107.
(81) Ona-Nguema, G.; Morin, G.; Wang, Y.; Juillot, F.; Abdelmoula, M.; Ruby, C.; Guyot, F.; Calas, G.; Brown, G. E. Arsenite sequestration by Fe(II)-containing minerals after microbial dissimilatory reduction


DOI: 10.1021/acs.est.5b04625
*Environ. Sci. Technol.* 2016, 50, 2281−2291

of arsenic-sorbed lepidocrocite. *Geochim. Cosmochim. Acta* **2009**, *73* (13), A973−A973.
(82) Lovley, D. R.; Coates, J. D.; Blunt-Harris, E. L.; Phillips, E. J. P.; Woodward, J. C. Humic substances as electron acceptors for microbial respiration. *Nature* **1996**, *382* (6590), 445−448.
(83) Jiang, J.; Bauer, I.; Paul, A.; Kappler, A. Arsenic redox changes by microbially and chemically formed semiquinone radicals and hydroquinones in a humic substance model quinone. *Environ. Sci. Technol.* **2009**, *43* (10), 3639−3645.
(84) Lovley, D. R.; Fraga, J. L.; Blunt-Harris, E. L.; Hayes, L. A.; Phillips, E. J. P.; Coates, J. D. Humic substances as a mediator for microbially catalyzed metal reduction. *Acta Hydrochim. Hydrobiol.* **1998**, *26* (3), 152−157.
(85) Amstaetter, K.; Borch, T.; Larese-Casanova, P.; Kappler, A. Redox transformation of arsenic by Fe(II)-activated goethite (alpha-FeOOH). *Environ. Sci. Technol.* **2010**, *44* (1), 102−108.
(86) Hudson-Edwards, K. A.; Houghton, S.; Taylor, K. G. Efficiences of As uptake from aqueous solution by a natural vivianite material at 4 degrees C. *Mineral. Mag.* **2008**, *72* (1), 429−431.


DOI: 10.1021/acs.est.5b04625
*Environ. Sci. Technol.* 2016, 50, 2281−2291